Laser Physics

Astro Ltd.

PAPER

Point-to-point conditioning of potassium dihydrogen phosphate (KDP) crystals combining sub-nanosecond and nanosecond ultraviolet lasers

To cite this article: Xiaofang Li *et al* 2019 *Laser Phys.* **29** 066001

View the article online for updates and enhancements.

This content was downloaded from IP address 130.237.165.40 on 30/04/2019 at 02:52

IOP Publishing | Astro Ltd Laser Physics
Laser Phys. **29** (2019) 066001 (6pp) https://doi.org/10.1088/1555-6611/ab1002

Point-to-point conditioning of potassium dihydrogen phosphate (KDP) crystals combining sub-nanosecond and nanosecond ultraviolet lasers

Xiaofang Li[1,2], Bo Wang[3], Dazhen Li[1,2], Houwen Yang[1,2] and Wenyong Cheng[1,4]

[1] Advanced Research Center for Optics, Shandong University, Shandong, Jinan 250100, People's Republic of China
[2] School of Information Science and Engineering, Shandong University, Shandong, Jinan 250100, People's Republic of China
[3] State Key Laboratory of Crystal Materials, Shandong University, Shandong, Jinan 250100, People's Republic of China

E-mail: cwy@sdu.edu.cn (W Cheng)

Received 14 July 2018, revised 8 March 2019
Accepted for publication 8 March 2019
Published 11 April 2019

Abstract

Laser-induced damage in potassium dihydrogen phosphate (KH_2PO_4 or KDP) crystals is a key limitation to inertial confinement fusion laser driver systems. To increase the laser damage resistance of KDP crystals, multi-parametric experiments with different fluence steps, shot numbers, starting fluences and pulse widths have been conducted to explore an optimum laser conditioning procedure. By employing a sub-nanosecond (sub-ns) laser and nanosecond (ns) laser collinear system at 355 nm, point-to-point conditioning and damage threshold testing of the KDP crystals were investigated. It is verified that conditioning by combining sub-ns and ns ultraviolet lasers can increase the laser-induced damage threshold of KDP crystals more efficiently. Thus, an optimized conditioning process combining sub-ns and ns lasers is proposed: first, irradiation with a sub-damage-threshold sub-ns laser is done to facilitate the recombination of conduction electrons and valence belt cavities; then, ns laser conditioning is performed to help with the regrowth of inclusions, plus the decomposition and regeneration of lattice structures.

Keywords: potassium dihydrogen phosphate (KDP) crystal, laser-induced damage, point-to-point, laser conditioning, damage induced threshold

(Some figures may appear in colour only in the online journal)

1. Introduction

Laser-induced damage in optical components, e.g. potassium dihydrogen phosphate (KDP) and its deuterated analog crystals, is a major challenge in the use of optical materials for various applications, extending from miniaturized optoelectronic devices to large-aperture laser systems for inertial confinement fusion [1, 2]. With the increase of laser-driver power, the problem of the laser-induced damage of KDP crystals becomes more significant. Since neither the improvement of crystal growing methods nor thermal annealing can meet the requirements of damage threshold in engineering, laser conditioning has been proposed to enhance the laser-induced damage threshold (LIDT) [3–6]. Compared with the former methods, laser conditioning is the best post-processing method to improve the LIDT of KDP crystals in a shorter

[4] Author to whom any correspondence should be addressed.

 © 2019 Astro Ltd Printed in the UK

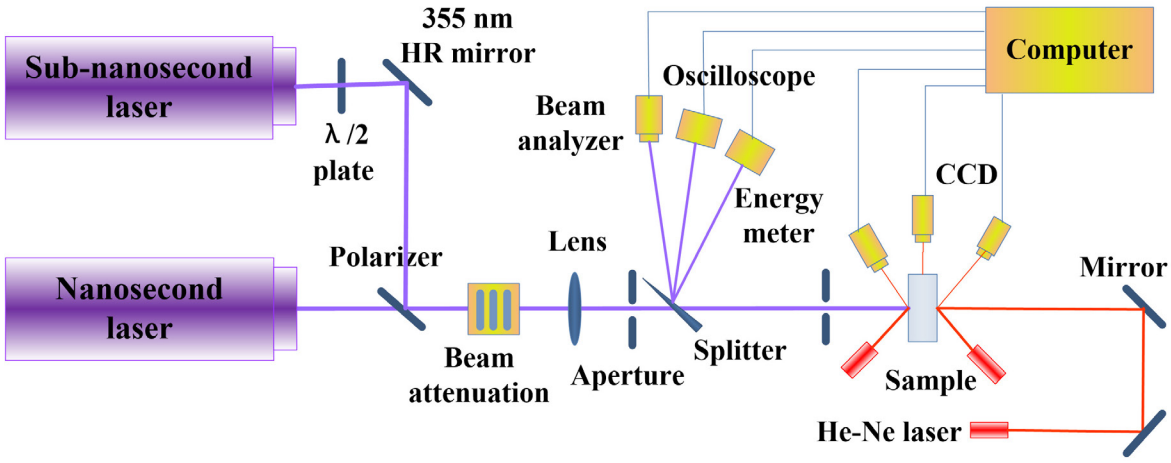

Figure 1. Experimental diagram of point-to-point conditioning and damage threshold testing system.

time. Besides, this process can be more targeted through its selective action on the local area of crystals. Laser conditioning is the last process for materials to run in the application, which can repair and control the residual defects in the processing of materials and the new defects after running in the application [7, 8].

In 1982, Swain *et al* proposed that the bulk laser-damage resistance of KDP crystals could be improved by pulsed laser irradiation [4]. In 2005, DeMange *et al* reported that the level of improvement can be achieved at various operational wavelengths of high-power lasers and found strong dependence of the effectiveness of laser conditioning on the conditioning wavelength [9]. In 2009, Zhao *et al* investigated the dependence of laser conditioning on the multiple process parameters and proposed a laser conditioning process by using a tripled nanosecond (ns) laser, which combined the N-on-1 and S-on-1 programs [10]. In 2012, Hu *et al* proposed that the local rapid-rising and slow-cooling process leads to the decrease of defect concentration, which can improve the laser damage resistance [11]. In 2015, Reyné *et al* investigated the morphology of bulk damages in KDP crystals induced by ns laser pulses, in particular by using three different wavelengths (1ω, 2ω and 3ω) [12]. Recently, Wang *et al* characterized the surface defects of KDP crystals and analyzed the influences of surface defects on laser-induced damage performances at 355 nm [13]. These findings suggested the methods of laser conditioning and the dependence of conditioning effects on some important factors, such as shot numbers, fluence steps, pulse wavelengths and so on. But the conditioning process that combines ultraviolet lasers with different pulse widths has not been proposed. Here, we propose a conditioning process that combines sub-ns and ns lasers.

To increase the efficiency and simplify the process of laser conditioning, we focus on the point-to-point conditioning of KDP crystals by setting up a collinear system employing a sub-nanosecond (sub-ns) laser and an ns laser both at 355 nm. Combining sub-ns and ns lasers, conditioning experiments with different fluence steps, shot numbers and starting fluences have been carried out. The experimental results indicate that the conditioning with sub-ns and ns lasers can increase the LIDT of KDP crystals more efficiently. In the optimized conditioning process, the sub-damage-threshold sub-ns laser irradiates on the crystals, which reduces the number of conduction electrons and makes the lattices more stable. After that, the ns laser conditioning mainly contributes to the regrowth of inclusions, plus the decomposition and regeneration of lattice structures.

2. Experiment

Figure 1 shows the setup of point-to-point conditioning and the damage threshold testing system. The light source is constituted of a sub-ns laser and an ns laser, both at 355 nm. The sub-ns laser with a pulse duration of 500 picoseconds is generated by an Nd:YAG laser (INNOLAS, SPITLIGHT AM SLM, Germany). The ns laser with a pulse duration of 6 ns is also delivered from an Nd:YAG laser (Powerlite DLS 8000, Continuum, USA).

The sub-ns and ns lasers are both horizontally polarized. A half waveplate rotates the sub-ns laser's polarization direction from horizontal to vertical. High-reflectance mirrors at 355 nm are adjusted to implement the perpendicularity of sub-ns and ns lasers. The polarizer is of high transmittance for a horizontal polarized laser, but high reflectance for a vertical polarized laser. Thus, the high transmittance of a horizontal polarized ns laser and the high reflectance of a vertical polarized sub-ns laser are achieved. With the half waveplate, high-reflectance mirrors and the polarizer, the sub-ns and ns laser paths are adjusted to collineation. An energy attenuator consists of a half waveplate and a polarizer. This is installed in the beam path to provide energy control. Then the beam is focused on the sample through the focusing lens with a focal length of 2000 mm. A wedge is used to pick up a portion of the beam to the diagnostics system including an energy meter (PE50BF-DIF-C, Ophir, Israel)) and a laser beam analyzer (SP620U, Ophir-Spiricon Corporation, USA). The measuring accuracy of the energy meter is 10^{-3} mJ and the area of each pixel in the laser beam analyzer is 4.4 μm $\times$ 4.4 μm. The effective areas of the sub-ns and ns laser spots focused on the sample are measured at ~0.03 mm^2 and ~0.07 mm^2, respectively.

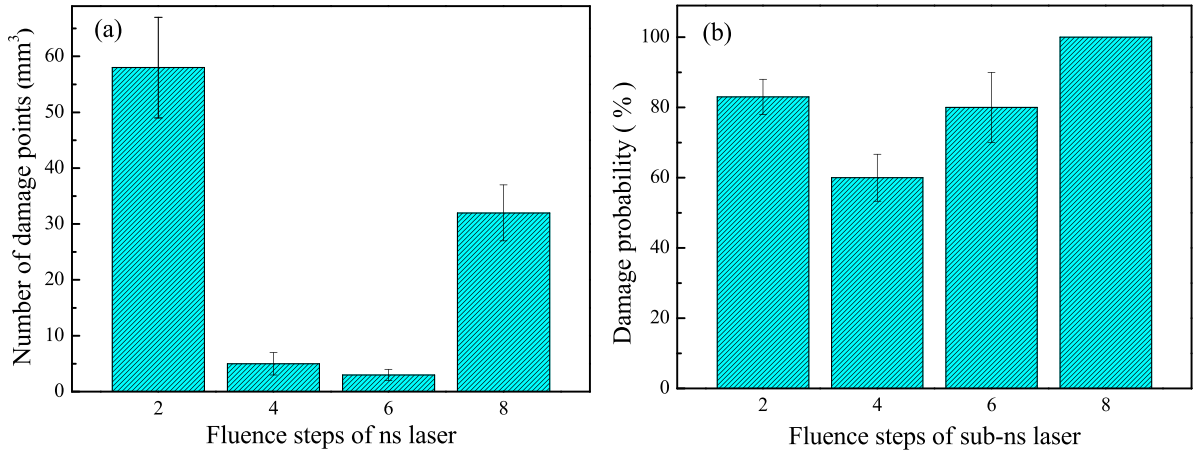

Figure 2. The bulk damage density and damage probability as a function of fluence steps, (a) ns laser, (b) sub-ns laser.

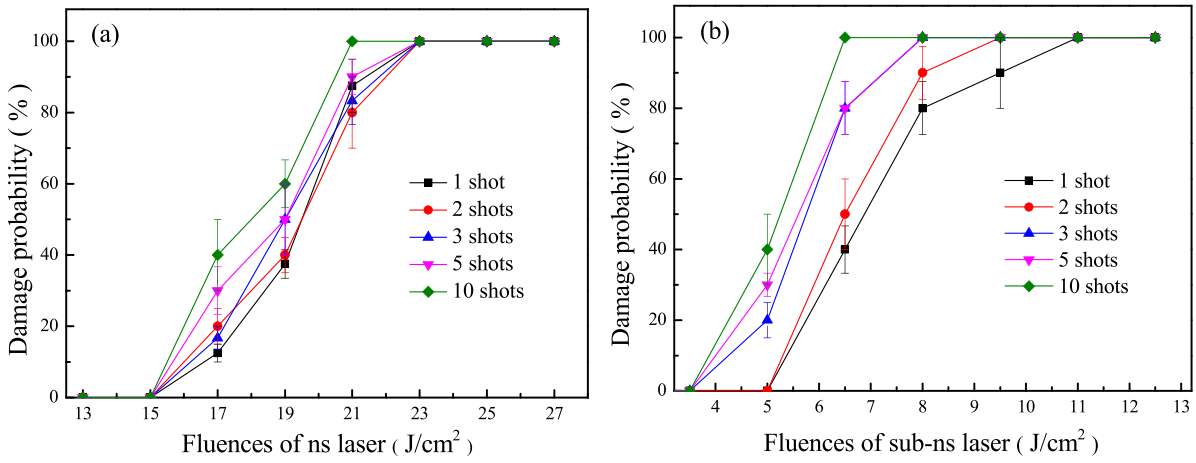

Figure 3. The bulk damage probability as a function of pulse numbers, (a) ns laser, (b) sub-ns laser.

The pristine KDP crystals are cut into $40 \times 40 \times 10\,\mathrm{mm}^3$ with type-II phase matching ($\theta = 58.6°$ and $\varphi = 0°$ at 298 K), and hand-polished on the front surface, the back surface and a side surface. The bulk damage of the samples is illuminated by using a counter-propagating continuous-wave He–Ne laser diagnostic beam. A CCD camera is used to capture the scattered light images of the bulk damage region through the polished side of the sample; orthogonally to the laser propagation direction. First, single-shot damage tests in the KDP samples with ns and sub-ns lasers are performed. Then, the KDP samples are pre-irradiated by conditioning pulses at different conditioning procedures, followed by the damage tests. The results are mainly represented as damage probability curves with error bars corresponding to 68% confidence [14]. In the end, morphology modifications of KDP samples are assessed by scanning electron microscopy (SEM).

3. Results and discussion

The KDP crystals are irradiated first by the laser with a gradually increasing fluence step-by-step on N-on-1 mode [10]. Then, the laser damage resistance of the conditioned KDP crystals is measured by using the 1-on-1 mode. The conditioning effect of the ns laser with different irradiation fluence steps is investigated with a damage pinpoint density [15]. The damage pinpoint density is measured over a volume of ~1 mm^3, which represents the bulk damage region of the KDP crystal exposed to the He–Ne laser. Specifically, when the ns laser irradiates on crystals, the bulk damage image observed by CCD shows discrete points. As for sub-ns laser, the damage image resembles a channel. Considering the bulk damage morphologies, the damage probability is used to assess the conditioning effects of sub-ns lasers. Figure 2 gives the conditioning results of the sub-ns and ns lasers with different fluence steps. As shown in figure 2(a), the damage pinpoint density of the ns laser with six fluence steps (1 J cm^{-2}, 3 J cm^{-2}, 5 J cm^{-2}, 7 J cm^{-2}, 9 J cm^{-2}, 11 J cm^{-2}) is lower than the others. Figure 2(b) shows that the damage probability of the sub-ns laser with four fluence steps (0.5 J cm^{-2}, 2 J cm^{-2}, 3.5 J cm^{-2}, 5 J cm^{-2}) is lower than that with other fluence steps. Thus, the appropriate conditioning steps of ns and sub-ns lasers are six and four, respectively. These results indicate that an appropriate number of steps can improve the effect of conditioning, but too many steps could decrease the conditioning efficiency.

The KDP samples are irradiated by the conditioning laser with the same fluence steps. At each fluence step, the crystals are irradiated with a fixed number of shots (1, 2, 3, 5 or 10 shots). Then, the damage tests are performed. The data in figure 3(a) shows that the damage probability of the ns laser with one

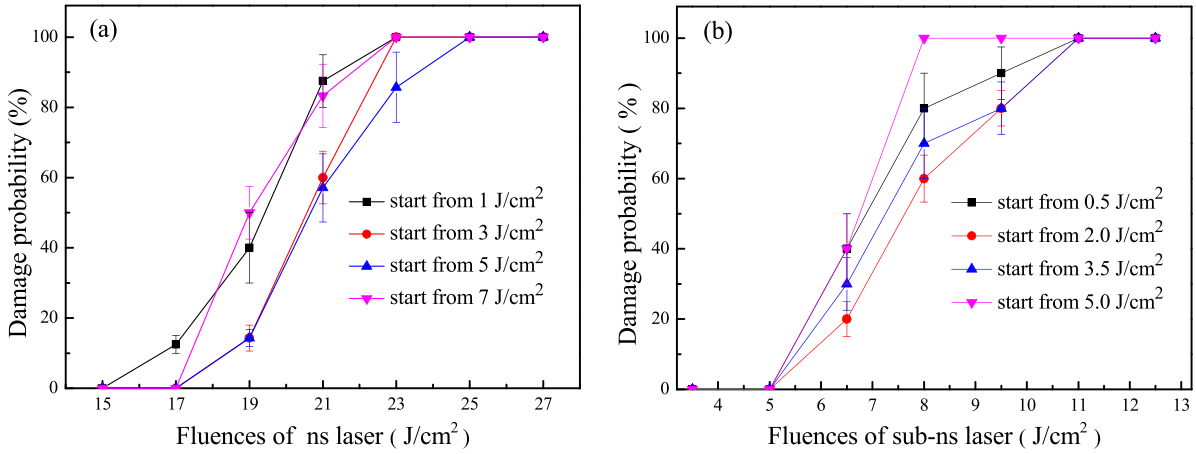
(a)
Damage probability (%)
start from 1 J/cm2
start from 3 J/cm2
start from 5 J/cm2
start from 7 J/cm2
Fluences of ns laser (J/cm2)
(b)
Damage probability (%)
start from 0.5 J/cm2
start from 2.0 J/cm2
start from 3.5 J/cm2
start from 5.0 J/cm2
Fluences of sub-ns laser (J/cm2)

Figure 4. The bulk damage probability as a function of starting conditioning fluence, (a) ns laser, (b) sub-ns laser.

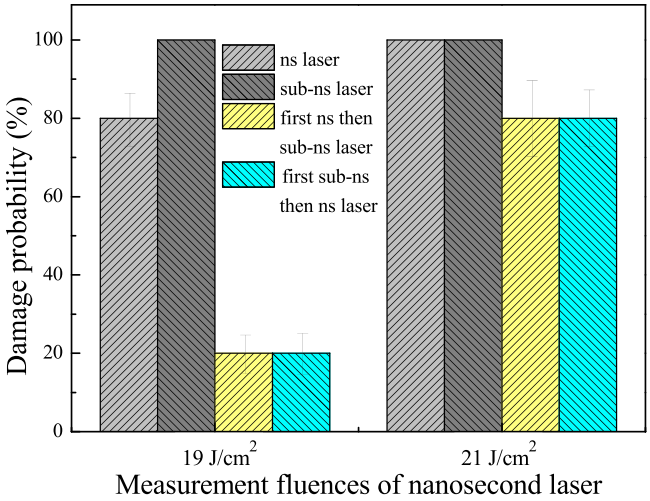

Figure 5. The bulk damage probability with ns and sub-ns lasers either or both by the 1-on-1 mode.

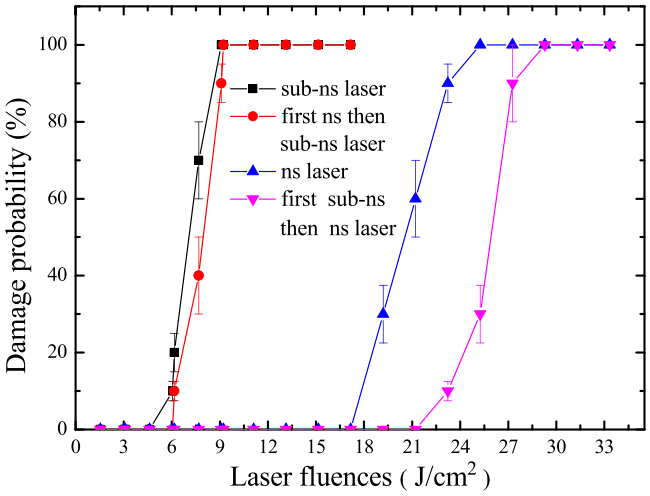

Figure 6. The bulk damage probability with the ns and sub-ns lasers either or both by R-on-1 mode.

shot is similar to that with two and three shots. Besides, the damage probability with ten shots is higher than the others. Figure 3(b) shows that the damage probability of the sub-ns laser with one shot is lower than those with more shots. The sub-ns laser conditioning effect is easier to be affected by the number of shots than the ns laser. These results indicate that an appropriate number of shots can improve the effect of conditioning, but too many shots may cost more time and decrease the conditioning efficiency.

Laser conditioning experiments with different starting irradiation fluences are performed. Then the damage threshold is tested with R-on-1 mode. The data in figure 4 shows that the crystals conditioned from the 5 J cm^{-2} by ns laser have the lowest damage probability, and crystals conditioned from 2 J cm^{-2} by the sub-ns laser have the lowest damage probability among the conditions tested. It is clear that effective conditioning needs appropriate starting fluences. The possible explanation is that changes will not occur in the surrounding material or the absorber before being heated up to the decomposition temperature or multi-photon ionization. In other words, laser conditioning effects mainly result from the relatively large conditioning fluence. The small conditioning fluence is not enough to decrease the defects of KDP crystals. Therefore, the maximal conditioning fluence is a key parameter to improve the damage resistance in laser conditioning [16].

The KDP crystals are pre-irradiated by ns, sub-ns, first ns and then sub-ns; and first by sub-ns then the ns laser, respectively. The bulk damage probability of the KDP crystals is then measured with a 1-on-1 mode in which the ns laser fluences are 19 J cm^{-2} and 21 J cm^{-2} at 355 nm. As shown in figure 5, the KDP crystals conditioned by combining sub-ns and ns lasers have a lower damage probability than those conditioned by one of the two lasers. This indicates that the combination of sub-ns and ns lasers can improve the conditioning effect.

We conduct the experiment where the KDP crystals are pre-irradiated by ns, by sub-ns, by the first ns then sub-ns, and by first sub-ns then the ns laser as well. The dependence of the conditioning effect is measured immediately by using the latter conditioning laser with the R-on-1 mode (figure 6). The LIDT of KDP crystals conditioned by the sub-damage-threshold sub-ns laser and then the ns laser is 1.375× higher than those conditioned only by ns laser (tested by the ns laser). Then the LIDT of the KDP crystals conditioned only by sub-ns laser is lower than that conditioned by the sub-damage-threshold ns laser and then the sub-ns laser (tested by the sub-ns laser).

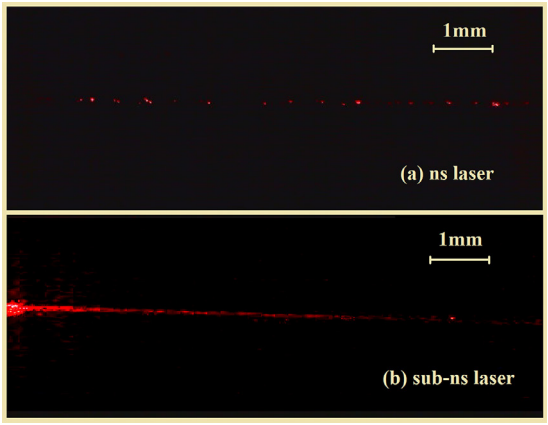

Figure 7. The CCD images of bulk damage in KDP crystals produced with ns and sub-ns laser pulses.

Therefore, the combination of the sub-ns and ns lasers shows a significant improvement on the conditioning effect.

Thus, the optimized conditioning process can be put forward. First, the sub-damage-threshold sub-ns laser conditioning is performed with the N-on-1 mode. Then, ns laser conditioning with maximum fluence—without causing damage—is adopted using the N-on-1 mode. The combined conditioning of sub-ns and ns lasers improves the LIDT dramatically.

The mechanisms of laser conditioning are analyzed, combining damage mechanisms and types of defect. When the KDP crystals are irradiated by the sub-ns laser, the damage changes from the electron avalanche breakdown to thermal effects [17, 18]. However, when the ns laser irradiates on KDP crystals, the main cause of the crystal damage is the thermal effect. The observed damage images in figure 7 can also verify our conclusion. When the ns laser irradiates on the crystal, the defects and laser self-focusing lead to uneven energy density, which results in damaged images with discrete points. The damage image of the sub-ns laser observed by a CCD resembles a channel, indicating that the interaction time between the sub-ns laser and KDP crystals is shorter, and multi-photon ionization causes the breakdown of KDP crystals. Moreover, due to the strong energy loss of the laser pulse in the front damage region, the bulk damage cavity is not performed throughout the crystal.

Bulk damage morphologies observed by the SEM are shown in figure 8. The laser-induced damage morphology shows the bulk damage cavity. Once the damage initiates, the shock wave and 'explosion' lead to a catastrophic increase in absorption at a high pressure or temperature, though the initial damage begins in regions less than about 100 nm in size [19]. The interaction time between the sub-ns laser and material is shorter, which results in much smaller cavity sizes in the damage site irradiated by the sub-ns laser, rather than being irradiated by the ns laser.

Similarly, the mechanisms of interaction between the KDP crystal and the laser at different pulse widths are different in the laser conditioning process. During the ns laser conditioning process, the initial defects of the crystal absorbs the laser energy, which leads to a rapid rise in the lattice temperature; and then gradual cooling for a long period, which is tens or hundreds of times longer than the rising time [20, 21]. This

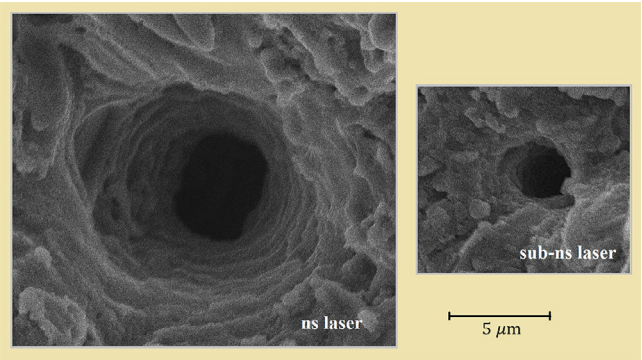

Figure 8. The SEM images of the damage sites in KDP crystals produced with ns and sub-ns laser pulses.

process resembles the process of thermal annealing. Thus, the ns laser mainly acts on large defects, such as structure defects or liquid inclusions. The size of the defects is commonly on the scale of 50 nm [22, 23]. Conditioning the laser leads to the melting of nanoparticles and the surrounding host lattices through the laser energy-absorption of the defects. Convection in the melt will then mix the defect with the surrounding material, or even the whole volume of the melt. After cooling, it requires a higher energy density to re-melt. Therefore, too many shot numbers and fluence steps have almost no effect on ns laser conditioning.

In the sub-ns laser conditioning process, a short thermal relaxation time of the micro inclusions, higher heating temperatures of the small micro inclusions and, accordingly, more effective annealing are achieved with a short pulse. However, aside from the thermal annealing, there were defects quenching in the sub-ns laser conditioning process. This quenching mainly aims at the defect in a relatively small size, which is mostly less than 50 nm, like with the electronic defect [22, 24]. Regarding the defect band-gap states that contribute to multi-photon ionization, the addition of electrons to atomic defects will remove the states within the band-gaps, thus reducing the transition probability. Through irradiation by a sub-damage-threshold laser, a sufficiently large density of electrons is liberated. The combined action of thermal annealing and defects quenching increases the LIDT of crystals. This explains why the effect of sub-ns laser conditioning decreases with too many shot numbers or fluence steps. Once the electronic defects recombine and disappear, further treatment increases the number of conduction electrons and decreases the stability of lattices. Then, in the presence of an internal temporal structure in the pulse, the cumulative effect associated with self-focusing also causes the drop of resistance when the crystals are irradiated with several pulses [25].

In the optimum conditioning process, the recombination of conduction electrons and valence belt cavities is realized when the sub-damage-threshold sub-ns laser irradiates on crystals. This reduces the number of conduction electrons and makes the lattices more stable. After that, the ns laser conditioning contributes to the regrowth of inclusions, the decomposition and regeneration of lattice structures. Thus, the combination of sub-ns and ns laser conditioning reduces the defect concentration, enhances the stability, and further improves the LIDT of crystals.

Experiments are carried out to verify the methods of laser conditioning with a small-aperture laser beam. But laser conditioning with a small-aperture beam for large-sized elements ($40 \times 40\,cm^2$, as in NIF) will take a long time. In engineering, the large-aperture crystals must be irradiated by a medium-aperture laser beam to increase the conditioning efficiency. However, the LIDT of crystals decreases with an increase in the beam aperture. This phenomenon is caused by the increased numbers of defects in the region irradiated by a larger-aperture beam and the nonuniformity of a larger-aperture beam. Due to the aperture-size effect on laser-induced damage, the laser conditioning with a medium-aperture beam imposes special requirements on a laser beam. A single frequency laser pulse is adopted to eliminate intensity peaks in the time domain. Besides, spatial intensity peaks in the spatial domain should be eliminated through spatial smoothing with spatial filters.

4. Conclusion

In this study, we set up a collineation system of a sub-ns laser and an ns laser, and carried out the point-to-point laser conditioning and damage threshold testing of the KDP crystals. Through laser conditioning experiments with different process parameters—such as fluence steps, shot numbers, starting fluences and pulse widths—we propose an optimized conditioning procedure, combining sub-ns and ns lasers. The sub-damage-threshold sub-ns laser conditioning is done first to quench the electronic defects. An ns laser conditioning process follows, with similar effects to thermal annealing. Thus, the combination of sub-ns and ns laser conditioning reduces the defect concentration, improves lattice stability, and further improves the LIDT of KDP crystals.

Acknowledgments

This work was supported by the Fundamental Research Funds of Shandong University (Grant No. 2015JC043), and the Independent Innovation Program of Universities and Institutes in Jinan City (Grant No. 201303007).

References

[1] Sheehan L, Kozlowski M, Rainer F and Staggs M 1994 *Proc. SPIE* **2114** 559–68
[2] Spaeth M L *et al* 2016 *Fusion Sci. Technol.* **69** 265–94
[3] Chen Y, Gao H, Wang X, Guo D and Liu Z 2018 *Materials* **11** 419
[4] Swain J, Stokowski S, Milam D and Rainer F 1982 *Appl. Phys. Lett.* **40** 350–2
[5] Swain J E, Stokowski S E, Milam D and Kennedy G C 1982 *Appl. Phys. Lett.* **41** 12–4
[6] Baisden P A *et al* 2016 *Fusion Sci. Technol.* **69** 295–351
[7] Batyreva I A, Bespalov V I, Kiselev A M and Miller A M 1978 *Sov. J. Quantum Electron.* **8** 1044
[8] Bredikhin V I, Ershov V P, Burenina V N, Mal'shakov A N and Potemkin A K 2007 *Quantum Electron.* **37** 489–94
[9] DeMange P, Carr C W, Negres R A, Radousky H B and Demos S G 2005 *Opt. Lett.* **30** 221–3
[10] Zhao Y A, Hu G H, Shao J D, Liu X F, He H B and Fan Z X 2009 *Proc. SPIE* **7504** 75041L
[11] Hu G, Zhao Y, Li D and Xiao Q 2012 *Opt. Express* **20** 25169
[12] Reyné S, Duchateau G, Hallo L, Natoli J Y and Lamaignère L 2015 *Appl. Phys.* A **119** 1317–26
[13] Wang S F, Wang J, Xu Q, Lei X Y, Liu Z C and Zhang J F 2018 *Appl. Opt.* **57** 2638–46
[14] Wagner F R, Hildenbrand A, Natoli J Y and Commandré M 2010 *Opt. Express* **18** 26791–8
[15] Zheng Y B *et al* 2017 *Opt. Laser Technol.* **96** 196–201
[16] Negres R A, DeMange P and Demos S G 2005 *Opt. Lett.* **30** 2766–8
[17] Carr C W, Radousky H B and Demos S G 2003 *Phys. Rev. Lett.* **91** 127402
[18] Duchateau G 2009 *Opt. Express* **17** 10434–56
[19] Carr C W, Matthews M J, Bude J D and Spaeth M L 2006 *Proc. SPIE* **6403** 64030K
[20] Wang X, Qin Y, Wang B, Zhang L, Shen Z H, Lu J and Ni X W 2011 *Appl. Opt.* **50** 3725–32
[21] Wang B and Gallais L 2013 *Opt. Express* **21** 14698–711
[22] Hu G, Zhao Y, Li D, Liu X, Zhu M and Shao J 2016 *Proc. SPIE* **10014** 100140M
[23] Liao Z M, Spaeth M L, Manes K, Adams J J and Carr C W 2010 *Opt. Lett.* **35** 2538–40
[24] Wang Y, Zhao Y, Hu G, Peng X, Chang J, Xie X, He J, Guo M and Shao J 2015 *Opt. Express* **23** 16273–80
[25] Belyaeva N N and Bredikhin V I 1984 *Sov. J. Quantum Electron.* **14** 433